AD-A151 004 STUDIES ON RADIATIVE COLLISIONAL AND ULTRAVIOLET LASERS 1/1
(U) STANFORD UNIV CA EDWARD L GINZTON LAB OF PHYSICS
S E HARRIS ET AL. DEC 84 GL-3812 AFOSR-TR-85-0134
UNCLASSIFIED F49620-83-C-0016 F/G 2/5 NL

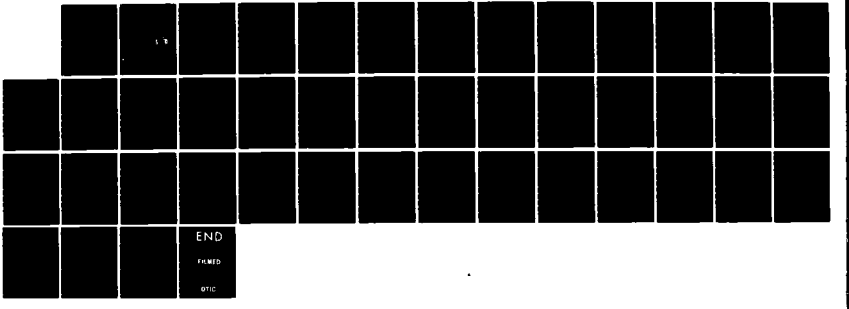

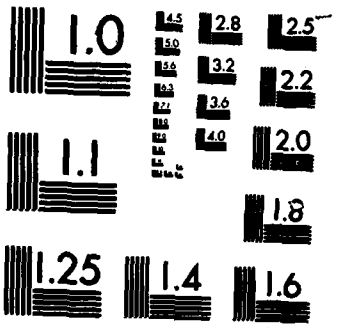

MICROCOPY RESOLUTION TEST CHART
NATIONAL BUREAU OF STANDARDS-1963-A

Report F49620-83-C-0016
Annual Technical Report
FQ8671-83-00204

G.L. Report No. 3812

STUDIES ON RADIATIVE COLLISIONAL AND ULTRAVIOLET LASERS

S. E. Harris
J. F. Young
Edward L. Ginzton Laboratory
W. W. Hansen Laboratories of Physics
Stanford University
Stanford, California 94305

December 1984

Annual Technical Report for Period 1 October 1983 - 30 September 1984

Contract Monitor:

Dr. Howard R. Schlossberg
AFOSR/NP
Bolling Air Force Base
Building 410
Washington, D.C. 20332

UNCLASSIFIED

SECURITY CLASSIFICATION OF THIS PAGE

REPORT DOCUMENTATION PAGE

1a. REPORT SECURITY CLASSIFICATION Unclassified	1b. RESTRICTIVE MARKINGS Unclassified
2a. SECURITY CLASSIFICATION AUTHORITY Unclassified	3. DISTRIBUTION/AVAILABILITY OF REPORT Approved for public release; distribution unlimited
2b. DECLASSIFICATION/DOWNGRADING SCHEDULE Unclassified	
4. PERFORMING ORGANIZATION REPORT NUMBER(S) G.L. 3812	5. MONITORING ORGANIZATION REPORT NUMBER(S) AFOSR-TR- 85-0134
6a. NAME OF PERFORMING ORGANIZATION Stanford University 6b. OFFICE SYMBOL (If applicable)	7a. NAME OF MONITORING ORGANIZATION Air Force Office of Scientific Research
6c. ADDRESS (City, State and ZIP Code) Edward L. Ginzton Laboratory Stanford, California 94305	7b. ADDRESS (City, State and ZIP Code) Bolling AFB, DC 20332
8a. NAME OF FUNDING/SPONSORING ORGANIZATION Air Force Office of Scientific Research 8b. OFFICE SYMBOL (If applicable) NP	9. PROCUREMENT INSTRUMENT IDENTIFICATION NUMBER F49620-83-C-0016
8c. ADDRESS (City, State and ZIP Code) Building 410 Bolling AFB, DC 20332	10. SOURCE OF FUNDING NOS. PROGRAM ELEMENT NO. 61102F; PROJECT NO. 2301; TASK NO. A1; WORK UNIT NO. N/A
11. TITLE (Include Security Classification) Studies on Radiative Collisional and Ultraviolet Lasers	
12. PERSONAL AUTHOR(S) S. E. Harris and J. F. Young	
13a. TYPE OF REPORT Annual Technical 13b. TIME COVERED FROM 10/83 TO 9/84	14. DATE OF REPORT (Yr., Mo., Day) December 1984 15. PAGE COUNT 41
16. SUPPLEMENTARY NOTATION Cont'd	
17. COSATI CODES FIELD / GROUP / SUB. GR.	18. SUBJECT TERMS (Continue on reverse if necessary and identify by block number) XUV Physics Laser Technology

19. ABSTRACT (Continue on reverse if necessary and identify by block number)

This program has supported theoretical and experimental studies in several areas of research on XUV physics and laser technology.

The highlight of our work during the previous year has been the definition and experimental confirmation of a new class of levels which we term as quasi-metastable. These levels allow significant simplification in our store and transfer methods and, of more importance, will, in certain cases, allow lasing in the extreme ultraviolet without the need for a transfer laser. Our work on these levels is summarized i

20. DISTRIBUTION/AVAILABILITY OF ABSTRACT UNCLASSIFIED/UNLIMITED ☒ SAME AS RPT. ☐ DTIC USERS ☐	21. ABSTRACT SECURITY CLASSIFICATION Unclassified
22a. NAME OF RESPONSIBLE INDIVIDUAL Howard R. Schlossberg	22b. TELEPHONE NUMBER (Include Area Code) (202) 767-4906 22c. OFFICE SYMBOL NP

DD FORM 1473, 83 APR EDITION OF 1 JAN IS OBSOLETE.

Unclassified

SECURITY CLASSIFICATION OF THIS PAGE

1. INTRODUCTION

This program has supported theoretical and experimental studies in several areas of research on XUV physics and laser technology.

The highlight of our work during the previous year has been the definition and experimental confirmation of a new class of levels which we term as quasi-metastable. These levels allow significant simplification in our store and transfer methods and, of more importance, will, in certain cases, allow lasing in the extreme ultraviolet without the need for a transfer laser. Our work on these levels is summarized in Appendices A and B of this report.

Section 2 of this report summarizes the status of our other projects, Section 3 lists the publications which have resulted under this contract, and Section 4 lists personnel who are presently supported by this contract.

Originator Supplied Keywords include:

See DD1473 (Block 18)

2. SUMMARY OF RESEARCH

A. Harmonic Generation for Probing the Cs 1091 Å Laser Transition

(K. D. Pedrotti and D. P. Dimiduk)

Computations of gain on the $Cs(5p^5 5d6s)^4P_{5/2} - (5p^6 6s)^2D_{5/2}$ transition have relied on measurements relating fluorescence intensity of the transition to the intensities of known Cs II (ion) lines. Measurements are made of the upper-state populations of the ion transitions by laser curve-of-growth techniques, as discussed in Section C. From these two measurements (and after accounting for radiation trapping effects), the population in the quasi-metastable $(5p^5 5d6s)^4P_{5/2}$ state can be inferred.

The accuracy of this calculation of the upper-state population in the 1091 Å laser depends on the Einstein A coefficients (radiative rates) of the two transitions. While experimental data is available on the transition strength in the ion, no such data is available on the 1091 Å transition. A project has been started to measure this transition strength by making high-resolution VUV absorption measurements at 1091 Å using laser techniques.

To make such an absorption measurement at 1091 Å it is desirable to have a tunable source of narrowband radiation at this wavelength. A technique which has been shown to be useful for generating radiation at these wavelengths is four-wave, sum-frequency mixing (4WSM). This nonlinear optical effect in gases produces radiation at the sum of the frequencies of three input waves. In the work referenced, a pulsed dye laser is pumped by a frequency-doubled 532 nm Q-switched dye laser. The output of the pulsed dye laser is frequency-doubled in a KDP crystal, creating radiation at a frequency $\omega_{UV} = 2\omega_{DYE}$. The two colinear beams coming out of the doubling

crystal (ω_{UV} and ω_{DYE}) are then focused together in a gas cell to make $\omega_{VUV} = 2\omega_{UV} + \omega_{DYE}$.

The work of Hilbig and Wallenstein showed tunable radiation could be generated via the 4WSM process in Kr between 1164 - 1100 Å. Wallenstein, in a private communication, indicated his calculations showed Kr to be negatively dispersive out to 1090.5 Å, and that his earlier experimental work was limited to 1100 Å by a MgF_2 window. We have duplicated Wallenstein's result in Kr and extended the tuning range to 1094.5 Å. At shorter wavelengths we find no evidence of sum-frequency generation. We find this roll-off in generation to be consistent with Kr becoming positively dispersive at 1094.5 Å, implying that the 4WSM process is not possible at shorter wavelengths in Kr. To check this hypothesis, small amounts of Ar (known to be positively dispersive at this wavelength) were mixed with the Kr, and the short wavelength edge of the sum-frequency generation process was noted to shift monotonically towards longer wavelengths, as expected.

After reviewing the literature and further calculations, Zn vapor was felt to be the next most suitable media for 4WSM at 1091 Å. A Zn heat pipe (cell) has been constructed and inserted into the previous experimental setup in place of the Kr cell. Generation of radiation tunable about 1091 Å has been observed. Unlike the earlier work of Stoicheff, et al. (using resonant mixing), these experiments were performed using non-resonant 4WSM. Generation efficiencies observed to date appear barely adequate for the absorption measurements in Cs. Further improvements may be possible by adding a suitable buffer gas to phasematch the Zn, which is probably excessively negatively dispersive at this wavelength. Using the same apparatus, it is possible to generate 1084 Å radiation with 4000 times more

efficiency because this generated wavelength corresponds to tuning the doubled-dye wavelength to the 10s two-photon resonance in Zn. This indicates large quantities of 1091 Å radiation could be generated by adding a second dye laser to the present experiment. In such an experiment, the first dye laser would be doubled and then tuned to the 10s two-photon resonance. The second dye laser would then be tuned such that the resultant three-photon sum frequency would correspond to 1091 Å. Although not being currently pursued due to the additional experimental complexity, this method could be important if it is necessary to generate an intense probe for single-pass gain measurements on the Cs laser transition.

B. Development of a Fast Transverse Alkali Atom Discharge

(D. A. King)

The number density of Na atoms in metastable and quasi-metastable levels produced by electron excitation in a pulsed hollow-cathode discharge (HCD) has recently been measured. These populations proved to be too small to build a Na based XUV laser in the HCD, so a new, relatively cheap and compact device for generating larger number densities of hot electrons was required. The device that seemed most suitable was a pulsed transverse discharge (PTD). This is the type of discharge commonly employed in N_2, metal vapor, and TEA lasers. The advantages of a PTD are that it has a much lower inductance than a HCD which, when applied with an improved driving circuit, produces larger peak voltages and currents in a shorter pulse. This gives rise, theoretically, to an order of magnitude increase in hot electron density over the hollow cathode. A transverse discharge cell was constructed with several different electrode configurations. Due to several experimental problems, however, both the cell and the circuit have had to be redesigned. After the recent proposal for a VUV laser in Cs, it was decided that the second PTD cell, now under construction, would be designed to experimentally demonstrate this laser.

The basic driver circuit is shown in Fig. 1 and worked as follows. Initially, a high-voltage dc power supply charged the charging capacitor (70 nF) through a balast resistor (30 kΩ) to about 30 kV. When the capacitor was fully charged the switch was closed, forming an RLC circuit with a small time constant (~ 150 ns) which acted to charge the peaking capacitors (20 nF). When the voltage across the gap reached a critical level the gap broke down, discharging the peaking capacitors. Although in

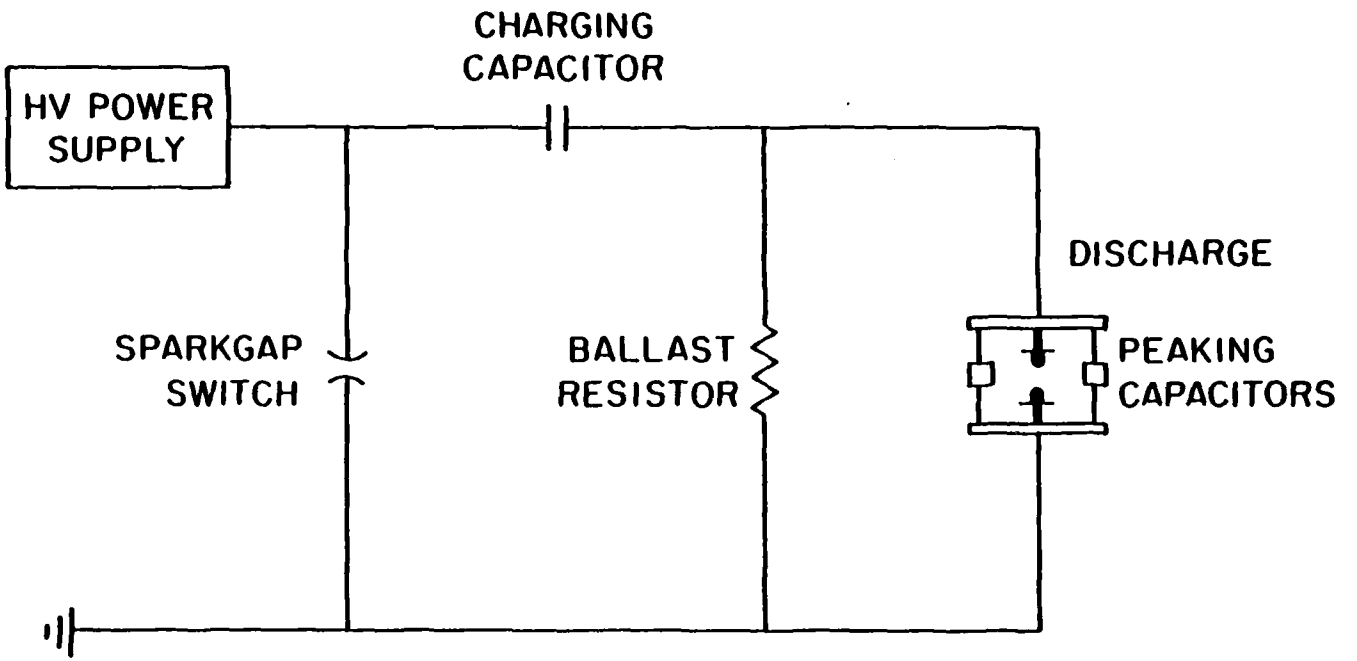

Fig. 1--Circuit diagram of the fast transverse discharge.

experiments this circuit produced a voltage pulse across the gap with a relatively fast rise time (70 - 100 ns), the gap broke down before the peaking capacitors were fully charged. The reason was that the voltage rise time across the capacitors was not fast enough due to the relatively large inductance of the switch (~ 200 nH). To solve this problem we have added an extra charging capacitor and a low inductance (~ 20 nH), self-triggering railgap switch.

The latest PTD cell consisted of a 90 cm long stainless steel cylinder, 38 cm in diameter, sealed at both ends. This cylinder acted as a vacuum vessel. It was evacuated and filled with typically less than 10 torr of buffer gas (usually He). The electrodes were thin stainless steel rods with an effective length of ~ 10 cm. The electrodes were placed parallel and separated by ~ 2 cm in a cylinder of compressed alumina (6 cm x 70 cm) which acted as a heat pipe. The cylinder rested on a brass plate which sat inside the vacuum vessel. Heaters were also placed inside the alumina cylinder. To minimize inductance the peaking capacitors were placed on the brass plate and a low-inductance feed geometry was used to connect them to the electrodes.

One of the main disadvantages of this design was that the optimum pressure of the He buffer gas was low enough that any gap whose electrode spacing was of the order of centimeters broke down easily. For instance, arcs formed by tracking across the peaking capacitors instead of across the main gap.

Following the proposal of a VUV Cs laser it was decided that an attempt would be made to make this laser in a PTD. With this in mind, the new cell design incorporates a compact, fused-silica vacuum vessel in the

form of a five-arm heat pipe. Two arms are used as voltage feeds in a low inductance geometry, another two arms parallel to the electrodes allow a laser beam to be passed through the discharge zone, and the fifth arm allows visual observation of the discharge. The problem of arcing is eliminated by placing the capacitors and heaters outside the vacuum vessel in air. This cell is now under construction.

If, by using the 1091 Å now being developed, we can experimentally demonstrate reasonable gain ($>> e^5$) at this wavelength then we will construct the Cs laser. Once we have emission at 1091 Å it will be used as a source for nonlinear optical experiments in the VUV and XUV. The experimental demonstrations of the Cs laser would also reinforce the concept of quasi-metastability, which is of fundamental importance in the proposed XUV Na laser.

C. Studies of the 1091 Å Transition In Neutral Cs

(J. K. Spong)

Theoretical and spectroscopic analysis described elsewhere in this report has identified the $(5p^5 5d6s)^4P_{5/2}$ - $(5p^6 5d)^2D_{5/2}$ transition in atomic Cs as a favorable candidate for the demonstration of VUV laser action at 1091 Å. Populations as large as 3 x 10^{11} atoms/cm^3 have been excited to the upper level of this transition by use of a hollow-cathode discharge. While no population inversion was present under the conditions of that work, in this section of the report we discuss preliminary experiments aimed at producing an inversion on the $^4P_{5/2}$ - $^2D_{5/2}$ transition, and eventually observing VUV laser action at 1091 Å.

In order to characterize the Cs plasma created by the hollow-cathode discharge, measurements were made of the populations in the $(5p^5 5d6s)^4P^0_{5/2}$ and $(5p^6 5d)^2D_{5/2}$ levels of neutral Cs and the $(5p^5 6s)(3/2)[3/2]^0_2$ and $(5p^5 5d)^3P^0_1$ levels of Cs^+. Populations were measured using the curve-of-growth technique described elsewhere, and typical discharge conditions resulted in populations of 3 x 10^{11} atoms/cm^3 in $Cs(5p^5 5d6s)^4P^0_{5/2}$, 10^{13} atoms/cm^3 in $Cs(5p^6 5d)^2D_{5/2}$, 10^{13} atoms/cm^3 in $Cs^+(5p^5 6s)(3/2)[3/2]^0_2$, and 5 x 10^{12} atoms/cm^3 in the $Cs^+(5p^5 5d)^3P^0_1$ level. In addition, the temperature and number density of the discharge electrons were measured. By measuring the Stark broadening of strong emission lines an electron density of 10^{14} electrons/cm^3 was inferred. The average temperature of this electron bath was measured by assuming electron equilibration of the populations in a Rydberg series, so that intensity ratios of optically-thin emission lines indicated the ambient electron temperature. Plots of emission intensity versus energy of the

Rydberg levels were fitted to a Boltzmann curve, and the temperature implied by the fit was 0.15 eV.

The dominant mechanism for populating the $(5p^6 5d)^2D_{5/2}$ lower laser level is electron excitation from the nearby $(5p^6 6p)^2P^o_{3/2}$ level. Using the electron temperature and density, we estimate the rate for this process to be 10^7/atom-sec. Since this is a factor of ten less than the rate at which the population can be removed by optical pumping with available laser power, it should be possible to achieve an inversion at 1091 Å in neutral Cs by first populating the upper $(5p^5 5d6s)^4P_{5/2}$ level and then emptying the lower level $(5p^6 5d)^2D_{5/2}$ by optical pumping to the continuum.

We have implemented this procedure in two ways. The first method used to dump the lower $^2D_{5/2}$ level was photoionization by the second harmonic of Nd:YAG radiation at 5320 Å. Using a tunable dye laser as a probe, the population of the lower level was observed to decline by a factor of 50 from its original density of 5×10^{13} *atoms/cm*^{3} with 80 mJ/cm^2 of incident laser energy.

An alternative technique used was to transfer population from the lower laser level to a Rydberg level, from which the electron ionization rate is rapid. From our temperature and density measurements, electron ionization rates were estimated to exceed 100 ps for Rydberg levels of the type nf, $n \geq 8$. Since the absorption cross section to such a Rydberg level exceeds that to the continuum by a factor of at least 100, this process allows use of a less-intense transfer laser. Using this technique, $(5d)^2D_{5/2} \rightarrow nf$ transitions were saturated with incident laser intensities only 10 - 50% of the photoionizing beam, depending on which Rydberg state was targeted.

The effectiveness of dumping lasers in emptying lower laser levels has thus been demonstrated. A systematic study of dumping techniques is planned with emphasis on enhancement of 1091 Å fluorescence and, finally, the observation of stimulated emission on the line as population inversion is achieved.

As a precursor to the proposed 1091 Å VUV laser, several visible laser schemes have been attempted using the Cs ion levels populated by the hollow-cathode discharge. Using the $Cs^+(5p^6 6s)(3/2)[3/2]_{J=2}$ metastable level as a storage state with a population of 10^{13} atoms/cm^3, a transfer laser was used to move the atoms into various $5p^5 6p$ levels, anticipating laser action down to levels in the $5p^5 5d$ configuration. Although emission on each of the proposed laser lines was enhanced by a factor of 100, there was no evidence that the emission was stimulated. Subsequent population measurements revealed densities of $4.5 - 8.0 \times 10^{12}$ atoms/cm^3 in each of the lower levels attempted, so that the necessary single-pass laser gain of e^{30} could not be achieved. Larger than expected populations in these $5p^5 5d$ levels were explained by Hartree-Fock calculations, which showed strong mixing of the $5p^5 5d$ configuration with the $5p^5 6s$ configuration. Calculated electron rates out of 5d were then dominated by an efficient electron ionization rate in from the Cs neutral ground state, keeping the $5p^5 5d$ levels substantially populated.

Although it does not appear possible to make a Cs^+ laser under present conditions, the experiment has led to a thorough characterization of the hollow-cathode environment and has disclosed the efficiencies with which discharge electrons fill and empty levels. These factors will be essential

in our attempts to create a population inversion on the $^4P_{5/2} - {}^2D_{5/2}$ 1091 Å transition.

D. XUV Emission Spectra of Core-Excited Levels in Na and Mg

(K. D. Pedrotti and A. J. Mendelsohn)

Emission spectroscopy is a powerful method for locating and identifying multiply-excited states with good radiative branching ratios. Such states are of great interest to us as both potential upper levels and storage levels for XUV lasers. We are particularly interested in finding quasi-metastable levels in the column I and II metals.

To accomplish this we have observed the XUV emission spectra of Na I and Mg II at much higher resolution than has been previously reported. Quasi-metastable levels have been observed in both species.

The experimental apparatus is shown in Fig. 2. The radiation source consists of a pulsed hollow-cathode discharge suspended in an all-metal heat pipe. The Mg spectra were taken at a pressure of 2 torr, a temperature of 600°C, and with an aluminum filter inserted between the discharge and spectrometer. The Na scans were taken at 500°C, 1 torr, and used a Ti-Sb-Ti filter. The discharge was run at a repetition rate of 100 Hz with a peak current of 100 A and a 4 μs duration. A McPherson 247, 2.2 m grazing-incidence monochromator equipped with a 30 ℓ/mm grating was used to gather the data. The output of our EMI D233 windowless electron multiplier was fed to photon-counting hardware and then to a Z-80 based microcomputer system for data collection and analysis.

The experimental results for Na between 365 and 415 Å are shown in Fig. 3. Table 1 lists the observed Na I features and Table 2 lists the remaining lines. The radiative and autoionizing rates in Table 1 were calculated using the RCG/RCN atomic physics code provided to us by

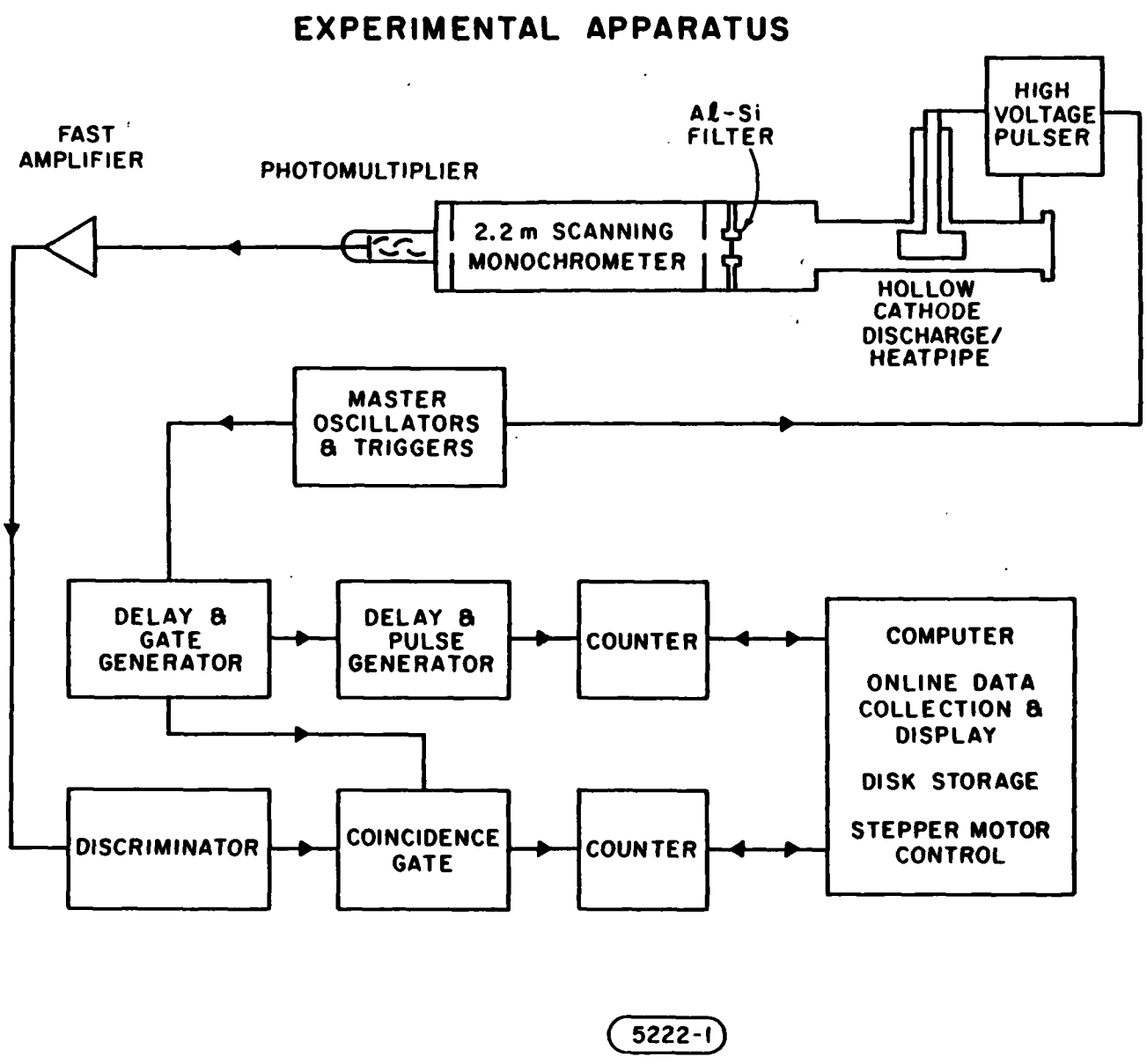

Fig. 2--Experimental apparatus.

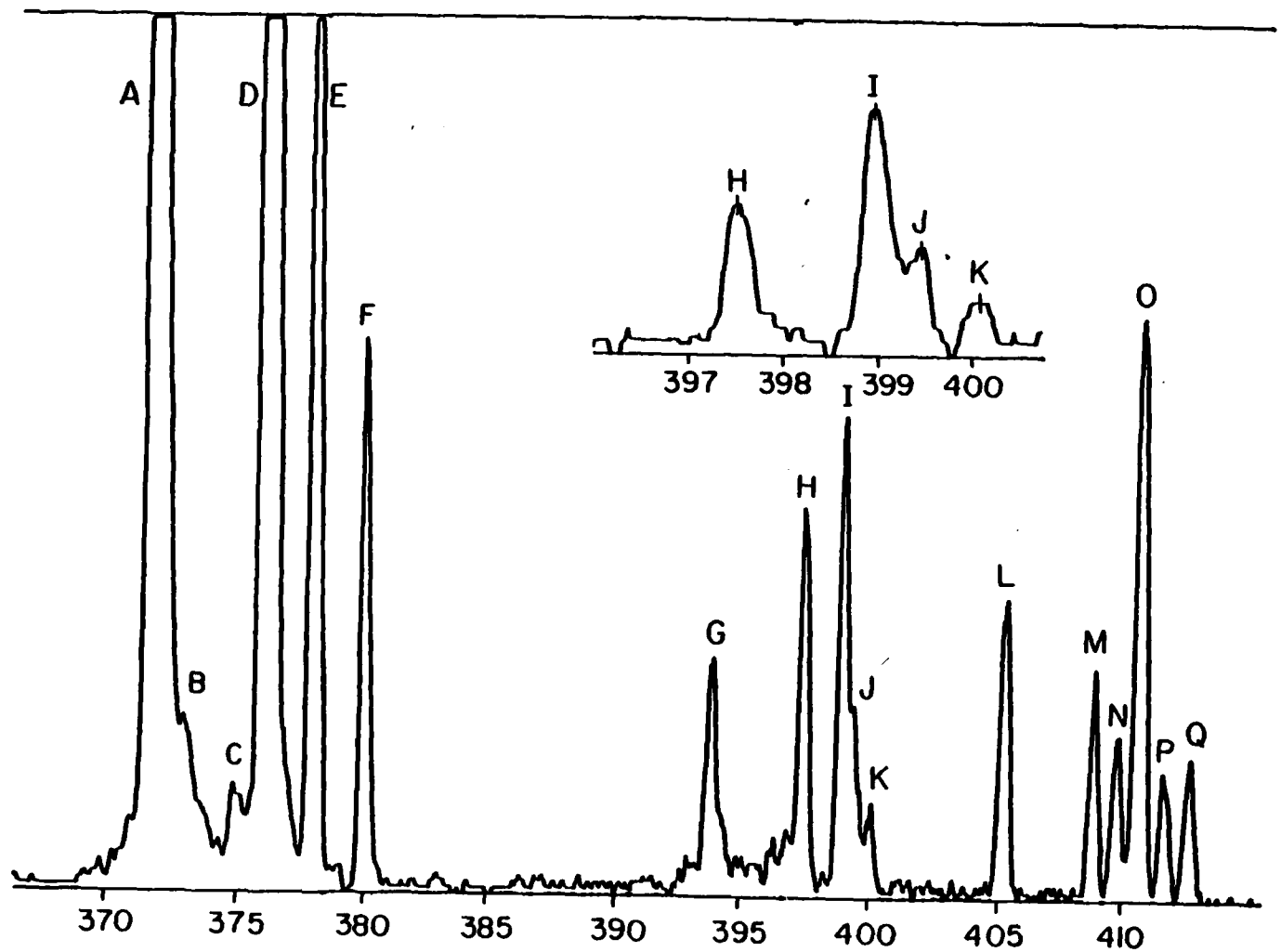

Fig. 3--Sodium XUV emission spectrum.

Table 1

Na I XUV Decays

Line	λ Experiment (nm)	λ Predicted (nm)	Identifications	Autoionizing Time (sec)	Radiative Rate (1/sec)	Intensity (counts)
C	37.514	37.50	$(2p^6 3d)\,^2P - [(2p^5 3s)\,^1P\ 3d]\,^2D_{3/2,5/2}$	3.0×10^{-11}	4.0×10^{9}	895
G	39.394	39.384	$(2p^6 3p)\,^2P - [2p^5(3s3p)\,^3P]\,^2P_{3/2}$	1.8×10^{-10}	1.4×10^{9}	113
H	39.752	39.7519	$(2p^6 3p)\,^2P - [2p^5(3s3p)\,^3P]\,^4P_{5/2}$	2.6×10^{-11}	2.3×10^{8}	282
I	39.898	39.9008	$(2p^6 3p)\,^2P - [2p^5(3s3p)\,^3P]\,^4D_{1/2}$	9.5×10^{-10}	1.0×10^{8}	338
J	39.942	39.9475	$(2p^6 3p)\,^2P - [2p^5(3s3p)\,^3P]\,^4D_{3/2}$	5.6×10^{-11}	1.4×10^{8}	152
K	40.014	40.0028	$(2p^6 3p)\,^2P - [2p^5(3s3p)\,^3P]\,^4D_{5/2}$	8.0×10^{-11}	7.4×10^{8}	64
L	40.526	40.5200	$(2p^6 3p)\,^2P - [2p^5(3s3p)\,^3P]\,^4S_{3/2}$	2.4×10^{-6}	9.6×10^{6}	190

Table 2

Other Na Decays

Line	λ Experiment (nm)	λ Predicted[a] (nm)	Identifications	Intensity (counts)
A	37.2074	37.2074	Na II $(2p^6)\,^1S_0 - 2p^5(^2P^o_{1/2})\,3s\,\frac{1}{2}\,[\frac{1}{2}]^o_{J=1}$	291,201
B	37.322	?	?	
D	37.6377	37.6377	Na II $(2p^6)\,^1S_0 - 2p^5(^2P^o_{3/2})\,3s\,\frac{3}{2}\,[\frac{3}{2}]^o_{J=1}$	492,168
E	37.814	37.8143	Na III $(2s^22p^5)\,^2P^o_{3/2} - (2s2p^6)\,^2S_{1/2}$	25,172
F	38.011	38.0107	Na III $(2s^22p^5)\,^2P^o_{1/2} - (2s2p^6)\,^2S_{1/2}$	12,502
M	40.868	40.8682	Na IV $(2s^22p^4)\,^3P_2 - (2s2p^5)\,^3P_1$	131
N	40.964	40.9615	Na IV $(2s^22p^4)\,^3P_1 - (2s2p^5)\,^3P_0$	93
O	41.043	41.0371	Na IV $(2s^22p^4)\,^3P_2 - (2s2p^5)\,^3P_2$	356
		41.0540	Na IV $(2s^22p^4)\,^3P_1 - (2s2p^5)\,^3P_1$	
P	41.144	41.1333	Na IV $(2s^22p^4)\,^3P_0 - (2s2p^5)\,^3P_1$	95
Q	41.237	41.2240	Na IV $(2s^22p^4)\,^3P_1 - (2s2p^5)\,^3P_2$	120

[a] From "Atomic and Ionic Emission Lines Below 2000 Å, R. L. Kelly and L. J. Palumbo, NRL Report 7599.

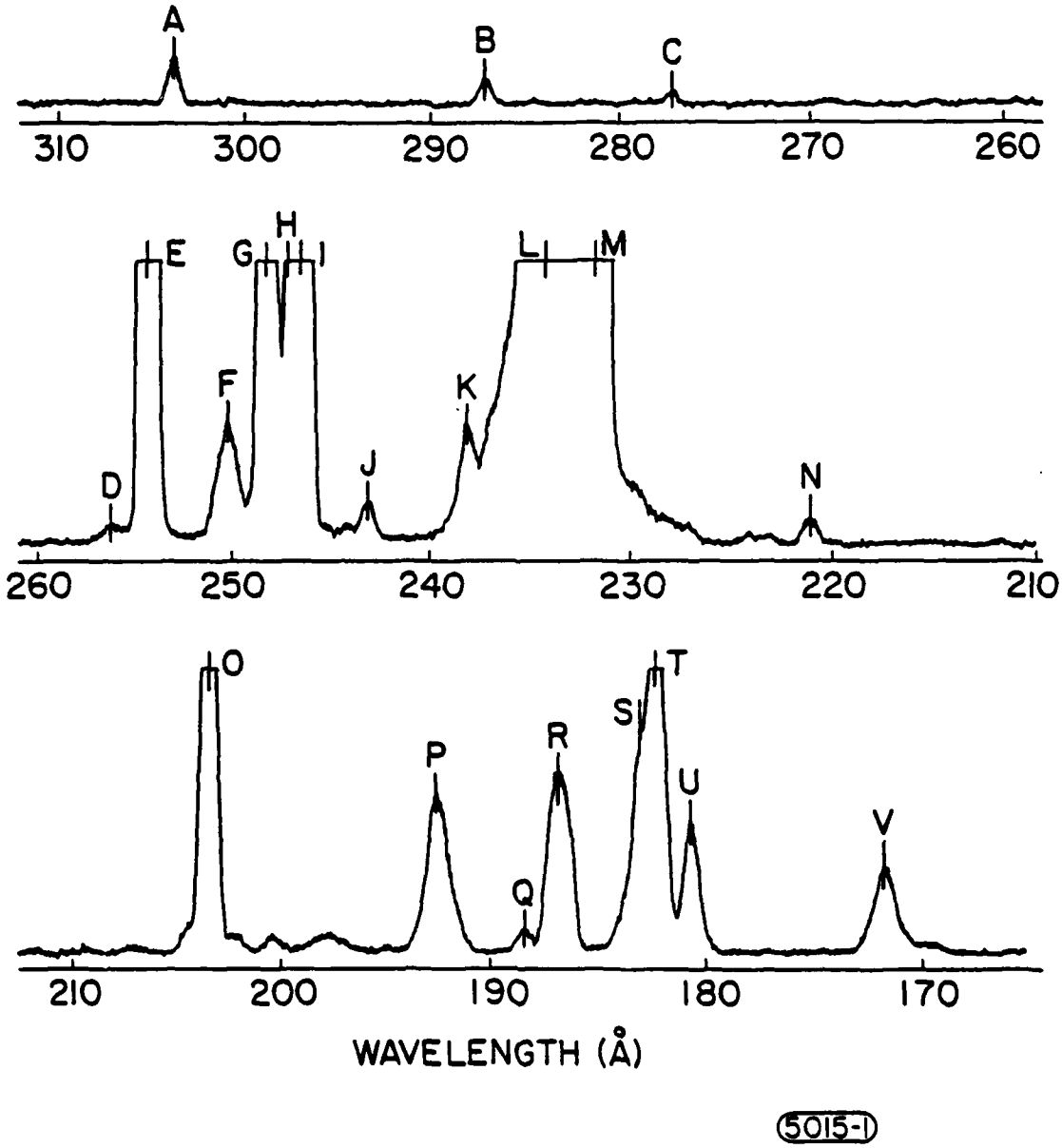

Fig. 4--Magnesium XUV emission spectrum.

Table 3

Mg II XUV Decays

Line	λ Experiment (nm)	λ Theory (nm)	λ Other Experiment (nm)	Identifications	Autoionizing Time (sec)	Radiative Rate (sec^{-1})	Intensity (arb. units)
B	28.71	28.72[d]	--	$(2p^6 4p)\,^2P - (2p^5 3s3p)\,^4S_{3/2}$	2.6×10^{-6} [a]	1.4×10^{4} [a]	2
C	27.72	27.73[d]	--	$(2p^6 4p)\,^2P - [(2p^5 3s)\,^1P]\ 3p\ ^2P_{3/2}$	1.0×10^{-9} [a]	2.2×10^{6} [a]	1
E	25.44	25.64[a]	25.42 [b]	$(2p^6 3p)\,^2P - (2p^5 3s3p)\,^4S_{3/2}$	2.6×10^{-6} [a]	2.1×10^{7} [a]	140
F	25.02	25.41[a]	25.04 [b]	$(2p^6 3p)\,^2P - (2p^5 3s3p)\,^4D$	1.3×10^{-10} [a]	7.0×10^{8} [a]	9
G	24.83	--	24.847[c]	$(2p^6 3s)\,^2S_{1/2} - (2p^5 3s^2)\,^2P^o_{3/2}$	3.3×10^{-13} [e]	2.6×10^{9} [e]	68
H	--	--	24.714[c]	$(2p^6 3s)\,^2S_{1/2} - (2p^5 3s^2)\,^2P^o_{3/2}$		1.2×10^{9} [e]	34
I	24.66	25.15[a]	24.66 [b]	$(2p^6 3p)\,^2P - [(2p^5 3s)\,^1P]\ 3p\ ^2P_{3/2}$	1.0×10^{-9} [a]	3.9×10^{9} [a]	95
K	23.81	24.14[a]	23.818[d]	$(2p^6 3d)\,^2D_{3/2} - 2p^5(3s4s\ ^3S)\,^2P^o_{1/2}$	2.0×10^{-10} [a]	2.15×10^{7} [a]	7
O	20.35	20.48[a]	20.353[c]	$(2p^6 3s)\,^2S_{1/2} - 2p^5(3s4s\ ^3S)\,^2P^o_{1/2}$	2.0×10^{-10} [a]	4.7×10^{8} [a]	43

[a] Hartree-Fock calculation using the RCN/RCG atomic physics code.

[b] Previously observed using projectile electron spectroscopy.

[c] Previously observed using absorption spectroscopy.

[d] Calculated using our experimental value for the upper level combined with values from NBS tables for the lower level.

[e] Previous theoretical calculation.

Table 4

Other Mg Lines Observed

Line	λ Experiment (nm)	λ Other Experiment (nm)	Identifications	Intensity (arb. units)
		Mg III		
L	23.42	23.426[a]	$(2p^6)\,^1S_0$ - $[(2p^5)\,^2P_{3/2}]$ 3s $^3P^o_1$	1250
M	23.18	23.173[a]	$(2p^6)\,^1S_0$ - $[(2p^5)\,^2P_{1/2}]$ 3s $^1P^o_1$	2150
Q	18.84	18.853[a]	$(2p^6)\,^1S_0$ - $[(2p^5)\,^2P_{3/2}]$ 3d $^3P^o_1$	1.5
R	18.70	18.720, 18.651[a]	$(2p^6)\,^1S_0$ - $(2p^5 3d)\,^3D_1$ and $^1P_1$	14.5
S	18.32	18.297[a]	$(2p^6)\,^1S_0$ - $[(2p^5)\,^2P_{3/2}]$ 4s $^3P^o_1$	28
T	18.24	18.224[a]	$(2p^6)\,^1S_0$ - $[(2p^5)\,^2P_{1/2}]$ 4s ^3P	2.3
V	17.18	171.89, 171.39, 170.81[a]	$(2p^6)\,^1S_0$ - $2p^5 4d$	7.0
		Mg IV		
U	18.09	18.079, 18.061[b]	$(2p^5)\,^2P$ - $(2p^4 3s)\,^2P_{1/2,3/2}$	11
V	17.18	17.165, 17.231[b]	$(2p^5)\,^2P$ - $(2p^4 3s)\,^2D_{5/2,3/2}$	7
		Other Lines		
A	30.38	30.378[c]	He II $(1s)\,^2S$ - $(2p)\,^2P^o$	4
D	25.63	25.632[c]	He II $(1s)\,^2S$ - $(3p)\,^2P^o$	1.5
J	24.31	—	Impurity	3
N	22.11	—	Magnesium	2
P	19.27	—	Magnesium	14

[a] Previous emission spectrum of Mg III.

[b] Previous emission spectrum of Mg IV.

[c] National Bureau of Standards tables.

R. D. Cowan. Figure 4 shows the spectrum of Mg between 310 and 170 Å. The Mg II XUV decays are listed in Table 3, with other lines shown in Table 4.

The most interesting decays are lines B and E in Mg II and line L in Na. These all arise from the $2p^5(3s3p^3P)^4S_{3/2}$ quasi-metastable level of each species. Line C in Na I and lines I and C in Mg II are important since they originate from doublet levels possessing good branching ratios and large radiative rates. This makes them attractive as upper levels for store and transfer XUV lasers.

E. XUV Lasers Using Super Coster-Kronig Decay

(A. J. Mendelsohn)

We have proposed a novel technique for making XUV lasers involving photoionization with laser plasma-produced x-rays and selective super Coster-Kronig decay into highly-excited states of Zn III.

The basic scheme is shown in Fig. 5. X-rays from a laser plasma photoionize ground-state Zn atoms maintained in a heat-pipe oven. (The proposed geometry is similar to that used by Caro and Wang in their Li photoionization experiments.) The resulting Zn II $3p^5 3d^{10} 4s^2$ ions undergo rapid super Coster-Kronig decay into the $3p^6 3d^8 4s^2$ configuration of Zn III where they preferentially populate the $(3d^8 4s^2)\,^1G_4$ level. Only ~ 10% of the decays from Zn II result in Zn III $3d^9 4s$ ions; hence, the super Coster-Kronig transition leaves the Zn III $(3d^8 4s^2)\,^1G_4$ level inverted with respect to levels in the lower Zn III configurations. By using tunable lasers to transfer the population in the $^1G_4$ level we may obtain inversion and superfluorescent lasing on the three transitions in Fig. 6.

The gain cross sections shown in Fig. 6 were calculated with the RCN/RCG atomic physics code. Using these values we calculate that a 1.06 μm pump laser energy of ~ 10 J should be sufficient to produce e^{20} gain on lasing on each of the transitions of Fig. 6 with an initial Zn ground-state density of $2 \times 10^{17}/cm^3$. This energy is within the range of the laser system currently being constructed under ONR support.

The Zn scheme has the following advantages compared to other similar proposals: (1) The super Coster-Kronig transition has a high branching ratio (60%) into the final $(3d^8 4s^2)\,^1G_4$ level, leading to large inversions in the lasing species; (2) the terminal laser levels lie > 70,000 cm^{-1} above the

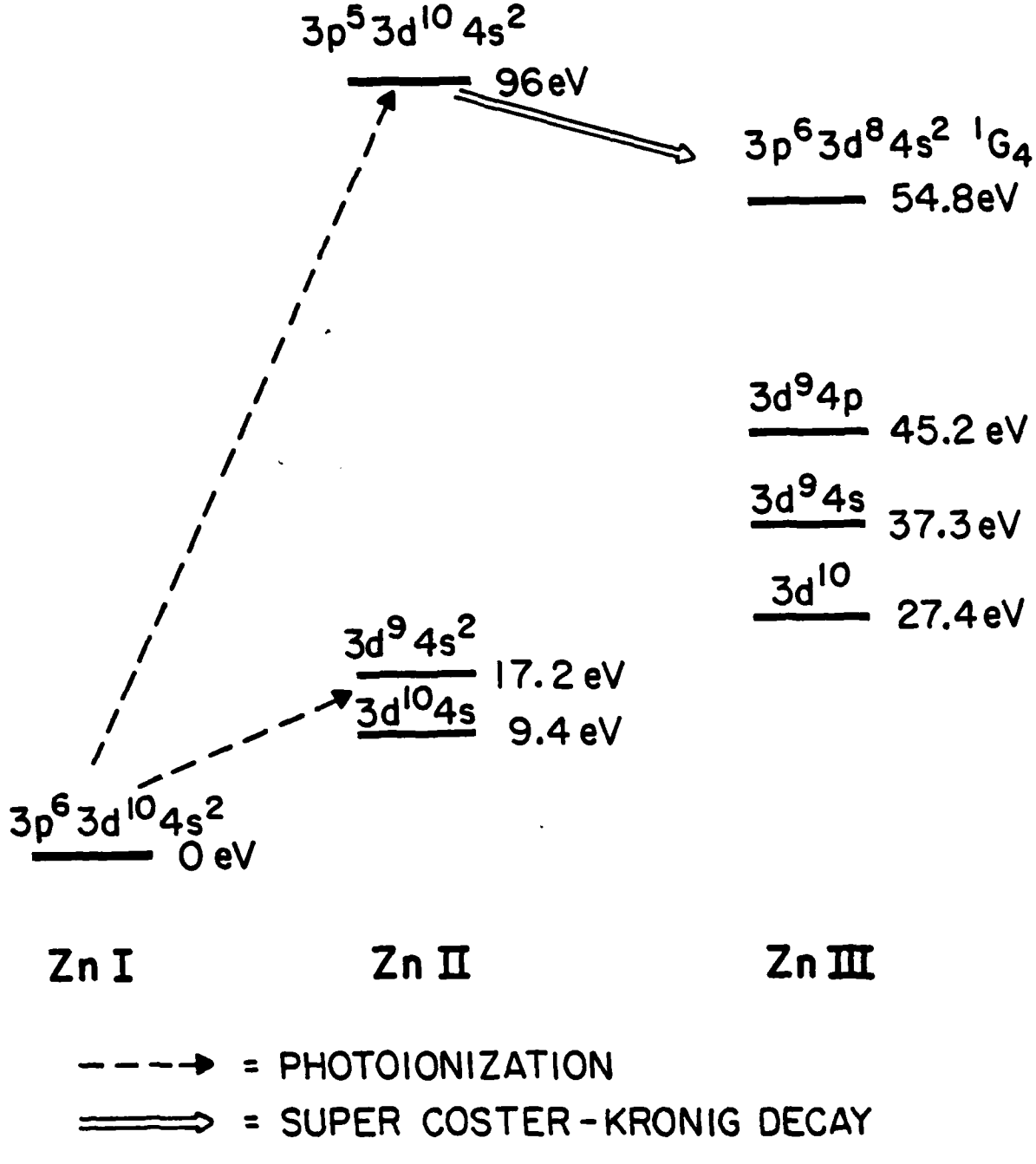

Fig. 5--Population of $(3d^8 4s^2)\,{}^1G_4$ level via super Coster-Kronig decay.

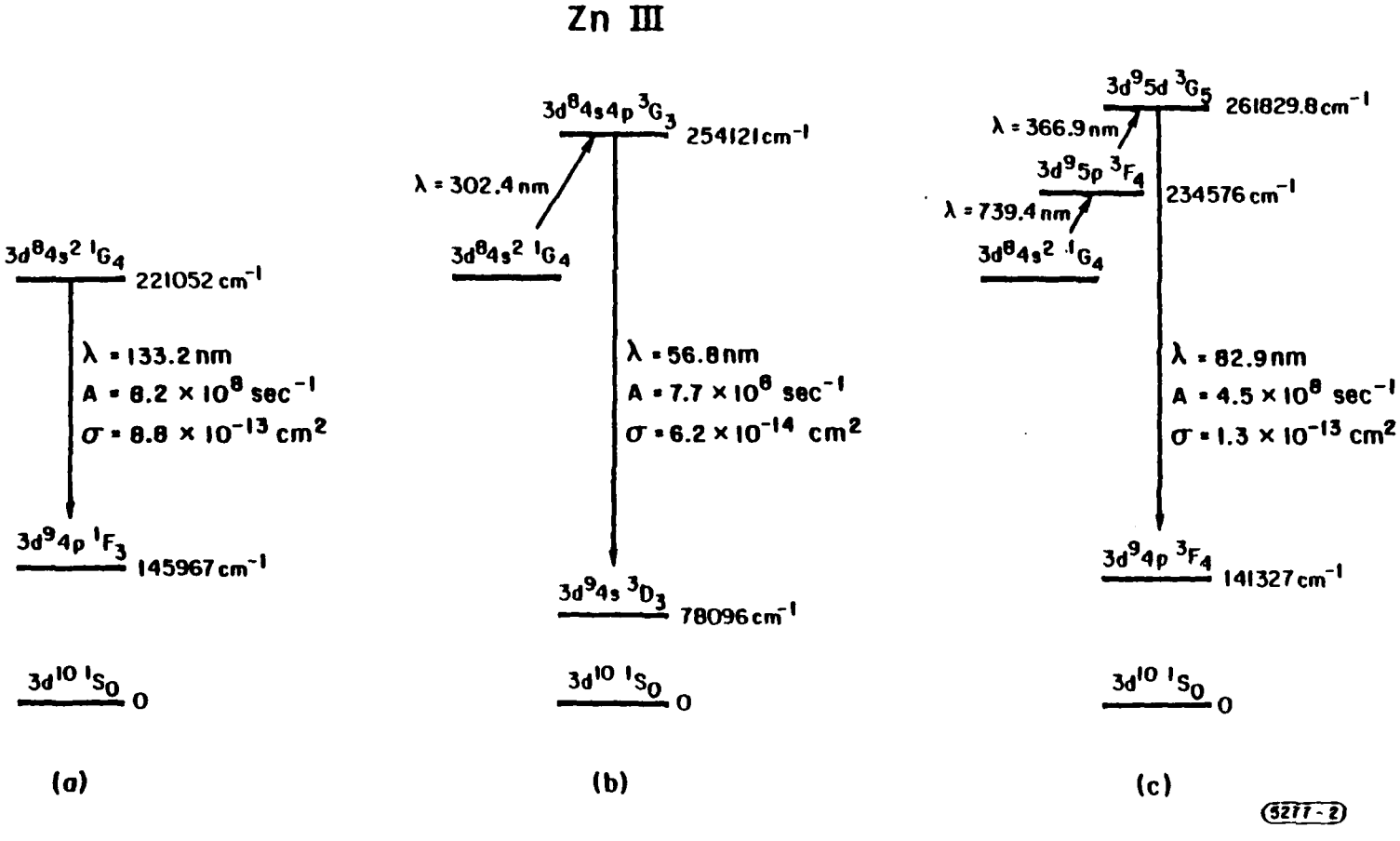

Fig. 6--Energy level diagrams for three possible laser systems in Zn III.

ground state of the lasing species and can only be populated by multistep electron impact processes; and (3) the initial species is neutral Zn vapor rather than a multiply-charged ion, as in other proposed Auger schemes. This allows the use of the simple heat pipe geometry already proven by Caro and Wang.

F. High-Resolution XUV Spectroscopy by Anti-Stokes Radiation

(D. P. Dimiduk)

A primary difficulty in using the broadly-tunable, anti-Stokes VUV light source for spectroscopy is the inherently low contrast of the source. The nature of the low contrast is that the spectroscopically useful anti-Stokes radiation is superimposed on spectrally nearby resonance-line radiation. Previous work used a monochromator as a bandpass filter to block the undesired background light from the resonance line. Since it is desirable to use the source to spectrally locate long-lived autoionizing states, and such states have absorption cross sections which are typically 1000 times as large as the background continuum cross section, it appears desirable to detect ejected electrons from the target species. Work on building a suitable fast electron detector began last year.

A fast, low-noise, parallel-plate electron detector was constructed. A parallel-plate type detector was chosen over an electron multiplier because it was felt that, given the observed absorption cross sections of the interesting states in K, the cell would need to operate at a pressure of 0.2 torr or more in order to absorb all of the available anti-Stokes photons. This is well above the operating range of an electron multiplier.

The detector's response speed was measured by applying a 5 ns pulse of 2660 Å laser light. At operating pressures of 0.5 torr or less, the detector response time was less than 20 ns. In this pressure regime, the detector speed is limited by electron velocity. In the alkalis investigated (Cs and K), electron transport at this pressure is a driven-diffusion phenomena. The observed detection speed agrees well with the calculated limiting velocities set by the applied E-field and known electron-atom

scattering cross sections. This time response is adequate for the intended application, where electrons are generated during laser pulses of approximately 5 ns.

The sensitivity of the fast-electron detector was measured using the same fast-pulse laser source. The photoionization cross section of the target atoms (Cs and K) are known at this wavelength, allowing calculation of the number of generated electrons in the detection cell. By carefully measuring the input intensity and comparing this to the time integral of the detector output current, the detector quantum efficiency could be measured. By attenuating the input light flux until the output signal was of the same mangitude as the noise, the absolute sensitivity of the detector was measured. The observed sensitivity (at an optimum bias voltage of 200 V) was approximately 3×10^5 electrons; the measured quantum efficiency was approximately 10%.

After comparing this observed sensitivity to the previously measured anti-Stokes source intensity it was concluded that, even with averaging, the detector did not have enough sensitivity to do new spectroscopy. In order to be spectroscopically interesting, an improvement in sensitivity of 10 - 30 would be required.

3. PUBLICATIONS

1. S. E. Harris, J. F. Young, R. G. Caro, R. W. Falcone, D. E. Holmgren, D. J. Walker, J. C. Wang, Joshua E. Rothenberg, and J. R. Willison, "Laser Techniques for Extreme Ultraviolet Spectroscopy," in Laser Spectroscopy VI, H. P. Weber and W. Luthy, eds. (New York: Springer-Verlag, 1983), pp. 376-381.
2. P. J. Wisoff and J. F. Young, "Active Mode-Locking of a Microwave-Pumped XeCℓ Laser," IEEE J. Quant. Elect. QE-20, 195-197 (March 1984).
3. D. E. Holmgren, R. W. Falcone, D. J. Walker, and S. E. Harris, "Measurement of Lithium and Sodium Metastable Quartet Atoms in a Hollow-Cathode Discharge," Opt. Lett. 9, 85-87 (March 1984).
4. S. E. Harris, D. J. Walker, R. G. Caro, A. J. Mendelsohn, and R. D. Cowan, "Quasi-Metastable Quartet Levels in Alkali-Like Atoms and Ions," Opt. Lett. 9, 168-170 (May 1984).
5. D. E. Holmgren, D. J. Walker, D. A. King, and S. E. Harris, "Grotrian Diagram of the Quartet System of Na I," in Laser Techniques in the Extreme Ultraviolet, S. E. Harris and T. B. Lucatorto, eds. (New York: AIP, 1984), pp. 157-161.
6. D. E. Holmgren, D. J. Walker, and S. E. Harris, "Emission at 1091 Å in Neutral Core-Excited Cs," in Laser Techniques in the Extreme Ultraviolet, S. E. Harris and T. B. Lucatorto, eds. (New York: AIP, 1984), pp. 496-501.
7. R. G. Caro, J. C. Wang, J. F. Young, and S. E. Harris, "X-Ray Excitation of Energetic Metastable Levels in Atoms and Ions," Opt. News (to be published).

8. S. E. Harris, R. G. Caro, R. W. Falcone, D. E. Holmgren, J. E. Rothenberg, D. J. Walker, J. C. Wang, J. R. Willison, and J. F. Young, "Metastability in the XUV: Lasers and Spectroscopy," in Proceedings of the Ninth International Conference on Atomic Physics, N. Fortson, ed. (Singapore: World Scientific Publishing Co.) (to be published).

9. D. E. Holmgren, D. J. Walker, D. A. King, and S. E. Harris, "Laser Spectroscopy of Na I Quartets," Phys. Rev. A (to be published).

10. A. J. Mendelsohn and S. E. Harris, "Proposal for an XUV Selective Autoionization Laser in Zn III," Opt. Lett. (to be published).

4. PERSONNEL

D. P. Dimiduk

S. E. Harris

D. E. Holmgren

D. A. King

A. J. Mendelsohn

K. D. Pedrotti

J. K. Spong

J. F. Young

APPENDIX A

Reprinted from Optics Letters, Vol. 9, page 168, May 1984

Quasi-metastable quartet levels in alkalilike atoms and ions

S. E. Harris, D. J. Walker, R. G. Caro, and A. J. Mendelsohn

Edward L. Ginzton Laboratory, Stanford University, Stanford, California 94305

R. D. Cowan

Los Alamos National Laboratory, Los Alamos, New Mexico 87545

Received January 5, 1984; accepted February 14, 1984

We describe the properties of a subclass of quartet levels of alkalilike atoms and ions that often retain metastability against autoionization and may have large radiative yields. Gain cross sections for XUV lasers with wavelengths between 20 and 100 nm are given.

It is well known that, in many cases, the quartet level of highest J of a given configuration of an alkalilike atom or ion is metastable against both autoionization and against radiation in the extreme ultraviolet (XUV). This occurs since, irrespective of the extent to which LS coupling holds, there is no doublet level in the configuration to which the quartet level may couple.[1]

In this Letter we note the existence of a subclass of quartet levels that, even in heavier elements, often retain relative metastability against autoionization and are radiatively allowed. In elements such as Cs and Ba these levels are candidates for the upper level of XUV lasers. In lighter alkalilike atoms and ions they provide storage levels for store and transfer lasers, which require orders-of-magnitude less transfer laser power than an earlier proposed Li system.[2]

The distinguishing property of these quasi-metastable levels is that the selection rules on the spin–orbit matrix elements allow nonzero matrix elements only to doublet basis levels, which are themselves prohibited from autoionizing. In second order, through the diagonalization, these levels do develop components of autoionizing doublet levels and therefore do autoionize, but often sufficiently slowly that the branching ratio for XUV radiation remains large.

To illustrate this idea, consider the $2p^5 3s 3p$ configuration of Na. First, the *pure* doublet levels that may not autoionize are $2p^5 3s 3p\ ^2P_{1/2,3/2}$; their doing so would not allow simultaneous conservation of parity and angular momentum. One then tabulates the possible quartet and doublet levels of this configuration: $^4S_{3/2}$, $^4P_{1/2,3/2,5/2}$, $^4D_{1/2,3/2,5/2,7/2}$, $^2S_{1/2}$, $^2P_{1/2,3/2}$, $^2D_{3/2,5/2}$. The pertinent selection rule on the spin–orbit element is $\Delta L = 0, \pm 1$. Therefore, of the possible quartet levels, those that couple only to the nonautoionizing $^2P_{1/2,3/2}$ levels are $^4S_{3/2}$ and $^4D_{1/2}$. We term these levels quasi-metastable.

Table 1 lists the quartet levels of the $2p^5 3s 3p$ configuration and their autoionizing rates as predicted by the atomic-physics code RCN/RCG,[3] with only this configuration included. Single and double stars in the left-hand column denote predicted quasi-metastability and metastability, respectively. The nonzero autoionizing rates of the quasi-metastable levels result from small components of autoionizing doublet levels, which are acquired in second order through the diagonalization. The code expansion of the quasi-metastable $2p^5 3s 3p\ ^4S_{3/2}$ level of Na is

$$^4S_{3/2} = 0.98\ ^4S_{3/2} - 0.15\ ^4P_{3/2} + 0.07(^1P)^2P_{3/2} + 0.04(^3P)^2P_{3/2} - 0.001(^1P)^2D_{3/2} - 0.001(^3P)^2D_{3/2}. \quad (1)$$

The $(0.001)^2$ components of $^2D_{3/2}$ result in the microsecond-time-scale autoionizing rate. The much larger $(0.07)^2$ component of $(^1P)^2P_{3/2}$ causes no autoionization and leads to a radiative rate of 7.7×10^6 on the transition $2p^5 3s 3p\ ^4S_{3/2} \rightarrow 2p^6 3p\ ^2P_{3/2}$ at 41.5 nm.

The quasi-metastable $^4D_{1/2}$ level lies higher in the configuration and couples more closely to nearby doublet levels. In second order it acquires a $(-0.014)^2$ component of $(^1P)^2S_{1/2}$, which in turn leads to its autoionizing rate of 2×10^9 sec^{-1}.

Table 2 tabulates the quasi-metastable quartet levels of all s,p,d configurations of the alkalilike atoms and ions. The requirement for quasi-metastability is summarized by $|J - L| = 3/2$; parity and angular momentum must be both even or both odd.

Table 3 tabulates the calculated single configurational autoionizing rate and dominant XUV radiation rate for the lowest-energy quasi-metastable level for the elements of columns I and II. In general, the selection

Table 1. Single Configurational Autoionizing Rates of Quartet Levels in the Sodium $2p^5 3s 3p$ Configuration

Level[a]	Autoionizing Rate (sec^{-1})
$^{**}4S_{3/2}$	6.06×10^5
$^4P_{1/2}$	10.1×10^{10}
$^4P_{3/2}$	4.5×10^{10}
$^4P_{5/2}$	2.67×10^{10}
$^{**}4D_{1/2}$	0.181×10^{10}
$^4D_{3/2}$	1.25×10^{10}
$^4D_{5/2}$	0.99×10^{10}
$^{***}4D_{7/2}$	0

[a] Single and double stars indicate predicted quasi-metastability and metastability, respectively.

0146-9592/84/050168-03$2.00/0

rule on quasi-metastability holds better and is less affected by the inclusion of other configurations for column I than for column II elements. As expected, it also tends to hold better in lighter elements and for low-lying levels.

We have made multiconfigurational code runs on several elements. In sodium, the inclusion of the $2p^53s3p$, $2p^53s4p$, $2p^53p4s$, and $2p^53p3d$ configurations changes the single configurational (Table 1) $2p^53s3p\ ^4S_{3/2}$ autoionizing rate to $4.1 \times 10^5\ sec^{-1}$ and the $2p^53s3p\ ^4D_{1/2}$ rate to $1.1 \times 10^9\ sec^{-1}$. In Ca^+ the inclusion of the $3p^53d4s$, $3p^54d4s$, $3p^55d4s$, and $3p^53d^2$ configurations changes the $3p^53d4s\ ^4P_{5/2}$ autoionizing rate (Table 3) to $1.03 \times 10^6\ sec^{-1}$. Ba^+ does particularly poorly. The $5p^55d6s$ and $5p^55d^2$ configurations are strongly mixed, and the autoionizing rate of the $^4P_{5/2}$ level can be made to vary between 10^{12} and 10^7, depending on the choice of the relative average energy of the two configurations.[4] On the other hand, Cs is relatively insensitive to the relative energy position and has a multiconfigurational autoionizing rate of $7.46 \times 10^7\ sec^{-1}$.

Radiation in the XUV has been observed and attributed to the $^4S_{3/2}$ and $^4P_{5/2}$ levels in several column I and column II metals by Aleksakhin *et al.*[5] and by Zhmenyah *et al.*[6] Also, a single configurational analysis by McGuire[7] predicts slow autoionizing rates for the $^4S_{3/2}$ levels of Na and Mg^+.

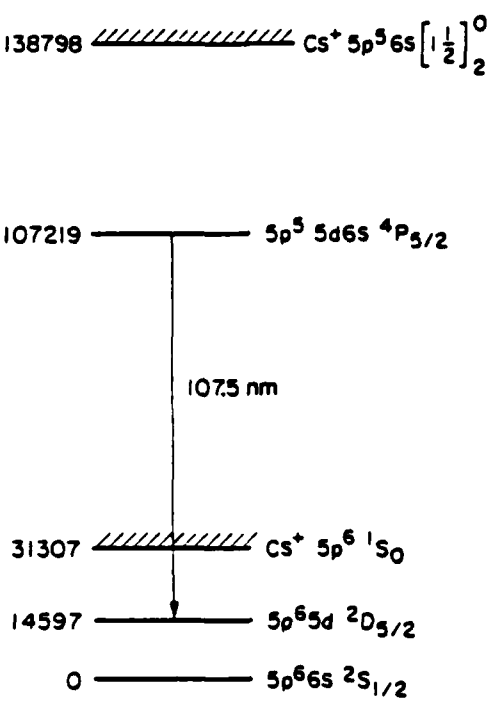

Fig. 1. Energy-level diagram for 107.5-nm Cs laser.

Table 2. Quasi-metastable Quartet Levels of Alkalilike Configurations

Configuration	Quasi-metastable Levels	Metastable Levels
p^5sp	$^4S_{3/2}$, $^4D_{1/2}$	$^4D_{7/2}$
p^5sd	$^4P_{5/2}$, $^4F_{3/2}$	$^4F_{9/2}$
p^5pd	$^4S_{3/2}$, $^4D_{1/2}$, $^4D_{7/2}$, $^4G_{5/2}$	$^4G_{11/2}$
p^5p^2	$^4P_{5/2}$	-
p^5d^2	$^4P_{5/2}$, $^4F_{3/2}$, $^4F_{9/2}$	-

Table table_3. Single Configurational Autoionizing and Radiative Rates for Quasi-metastable Column I and Column II Elements

Element	Upper Level	Autoionizing Rate	Radiative Rate	λ (nm)	Lower Level
Na	$2p^53s3p\ ^4S_{3/2}$	6.1×10^6	7.7×10^8	41.5	$3p\ ^2P_{3/2}$
K	$3p^53d4s\ ^4P_{5/2}$	4.6×10^2	3.0×10^8	71.1	$3d\ ^2D_{3/2}$
Rb	$4p^55s5p\ ^4S_{3/2}$	8.6×10^7	2.6×10^7	82.1	$5p\ ^2P_{3/2}$
Cs	$5p^55d6s\ ^4P_{5/2}$	5.1×10^7	4.1×10^7	107.5	$5d\ ^2D_{5/2}$
Mg^+	$2p^53s3p\ ^4S_{3/2}$	9.3×10^4	1.9×10^7	25.6	$3p\ ^2P_{3/2}$
Ca^+	$3p^53d4s\ ^4P_{5/2}$	9.3×10^5	4.1×10^8	52.9	$3d\ ^2D_{5/2}$
Sr^+	$4p^54d5s\ ^4P_{5/2}$	1.4×10^8	5.3×10^7	62.0	$4d\ ^2D_{5/2}$
Ba^+	$5p^55d6s\ ^4P_{5/2}$	2.7×10^9	8.8×10^7	77.1	$5d\ ^2D_{5/2}$

Table 4 gives the transition wavelength, Doppler width, and gain cross section σ for XUV laser transitions that originate from the lowest quasi-metastable level of each element. The Doppler width is calculated at a

Table 4. Gain Cross Sections of Transitions from Quasi-metastable Levels

Element	Transition	λ (nm)	Doppler Width (cm^{-1})	σ (cm^2)
Na	$2p^53s3p\ ^4S_{3/2} \rightarrow 2p^63p\ ^2P_{3/2}$	41.5	1.04	1.6×10^{-16}
K	$3p^53d4s\ ^4P_{5/2} \rightarrow 3p^63d\ ^2P_{3/2}$	71.1	0.43	4.4×10^{-16}
Rb	$4p^55s5p\ ^4S_{3/2} \rightarrow 4p^65p\ ^2P_{1/2}$	82.1	0.24	9.1×10^{-15}
Cs	$5p^55d6s\ ^4P_{5/2} \rightarrow 5p^65d\ ^2D_{5/2}$	107.5	0.15	3.9×10^{-14}
Mg^+	$2p^53s3p\ ^4S_{3/2} \rightarrow 2p^63p\ ^2P_{1/2}$	25.6	1.78	8.71×10^{-17}
Ca^+	$3p^53d4s\ ^4P_{5/2} \rightarrow 3p^63d\ ^2D_{5/2}$	52.9	0.83	1.72×10^{-16}
Sr^+	$4p^54d5s\ ^4P_{5/2} \rightarrow 4p^64d\ ^2D_{5/2}$	62.0	0.45	5.6×10^{-15}
Ba^+	$5p^55d6s\ ^4P_{5/2} \rightarrow 5p^65d\ ^2D_{5/2}$	77.1	0.27	2.4×10^{-14}

temperature corresponding to a vapor pressure of 10 Torr.

Figure 1 is an energy-level diagram for a 107.5-nm Cs laser. The $^4P_{5/2}$ level will be populated by electron collisions at a peak excitation cross section that Aleksakhin *et al.*[5] estimate as 5.8×10^{-17} cm^2 and also by charge transfer from the $Cs^+ 5p^5 6s$ ion. The lower laser level $5p^6 5d\ ^2D_{5/2}$ will also be excited by electron collisions but can probably be emptied by laser excitation to a Rydberg level or to the $Cs^+ 5p^6$ continuum.

Population in the quasi-metastable levels of the column II elements of Table 4 can be produced by soft-x-ray photoionization[8,9] of populated valence levels. For example, photoionization of atoms in the $5p^6 5d 6s\ ^4D$ level of Ba will produce $5p^5 5d 6s\ ^4P_{5/2}$ ions with a statistical branching ratio of about 7%. A possible advantage of using column II metals is that the lower laser level is an excited level of the ion rather than of the neutral.

The authors gratefully acknowledge helpful discussions with T. Lucatorto, A. W. Weiss, and P. J. K. Wisoff.

The research described here was supported by the U.S. Air Force Office of Scientific Research and the U.S. Army Research Office.

References

1. P. Feldman and R. Novick, "Autoionizing states in the alkali atoms with microsecond lifetimes," Phys. Rev. 160, 143 (1967).
2. S. E. Harris, "Proposal for a 207-Å laser in lithium," Opt. Lett. 5, 1 (1980); and J. E. Rothenberg and S. E. Harris, "XUV lasers by quartet to doublet energy transfer in alkali atoms," IEEE J. Quantum Electron. QE-17, 418 (1981).
3. R. D. Cowan, *The Theory of Atomic Structure and Spectra* (U. California Press, Berkeley, Calif., 1981), Secs. 8-1, 16-1, and 18-7.
4. J. P. Connerade, M. W. D. Mansfield, G. H. Newsom, D. H. Tracy, M. A. Baig, and K. Thimm, "A study of 5*p* excitation in atomic barium. I. The 5*p* absorption spectra of Ba I, Cs I and related elements," Phil. Trans. R. Soc. London Ser. A 290, 327 (1979); S. J. Rose, I. P. Grant, and J. P. Connerade, "A study of 5*p* excitation in atomic barium. II. A fully relativistic analysis of 5*p* excitation in atomic barium," Phil. Trans. R. Soc. London Ser. A 296, 41 (1980).
5. I. S. Aleksakhin, G. G. Bogachev, I. P. Zapesochnyl, and S. Yu. Ugrin, "Experimental investigations of radiative decay of autoionizing states of alkali and alkaline earth elements," Sov. Phys. JETP 53, 1140 (1981).
6. Yu. V. Zhmenyak, V. S. Vukstich, and I. P. Zapesochnyl, "Radiative decay of Na I autoionization states excited in electron–atom collisions," Pis'ma Zh. Eksp. Teor. Fiz. 35, 321 (1982).
7. E. J. McGuire, "The *L-MM* Auger spectra of Na and Mg," Phys. Rev. A 14, 1402 (1976).
8. R. G. Caro, J. C. Wang, R. W. Falcone, J. F. Young, and S. E. Harris, "Soft x-ray pumping of metastable levels of Li^+," Appl. Phys. Lett. 42, 9 (1983).
9. W. T. Silfvast, J. J. Macklin, and O. R. Wood II, "High-gain inner-shell photoionization laser in Cd vapor pumped by soft-x-ray radiation from a laser-produced plasma source," Opt. Lett. 8, 551 (1983).

APPENDIX B

EMISSION AT 1091 Å IN NEUTRAL CORE-EXCITED Cs

D. E. Holmgren, D. J. Walker, and S. E. Harris
Edward L. Ginzton Laboratory
Stanford University, Stanford, California 94305

ABSTRACT

Certain quartet levels in alkali-like systems retain metastability against autoionization while acquiring large radiative yields. This quasi-metastability occurs through selective coupling to non-autoionizing doublet levels by the spin-orbit interaction. An example of such a level is the $5p^5 5d6s\ ^4P_{5/2}$ level of neutral Cs, which has a calculated branching ratio for radiation at 1091 Å of 43%. Experimentally, we find that this line has an emission intensity equal to 1/6 of that of the strongest ion line of Cs^+, and is a promising candidate for an extreme ultraviolet laser.

INTRODUCTION

It has recently been noted[1] that a sub-class of quartet levels of alkali atoms and ions retain metastability against autoionization and may have large radiative yields. This quasi-metastability occurs through selective coupling to non-autoionizing doublet levels by the spin-orbit interaction. An example of such a level is the $5p^5 5d6s\ ^4P_{5/2}$ level of neutral Cs (Fig. 1). The atomic physics code[2] RCN/RCG predicts a branching ratio for radiation on the $5p^5 5d6s\ ^4P_{5/2} \rightarrow 5p^6 5d\ ^2D_{5/2}$ transition at 1091 Å of about 43%.

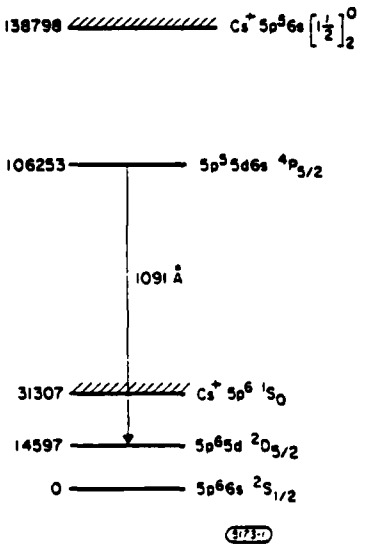

Fig. 1. Energy level diagram of Cs laser.

Experimentally, using a pulsed hollow-cathode discharge we find the ratio of emission on this line to the emission at 927 Å which results from the Cs^+ transition $5p^5 6s\ [1\frac{1}{2}]^0_1 \rightarrow 5p^6\ ^1S_0$ to be about 16%. Since the cross section for electron excitation of this latter transition is known, we may infer both a strong excitation and a good branching ratio for 1091 Å emission. Since the lower level of this transition, $5p^5 5d\ ^2D_{5/2}$, may be emptied by an incident laser beam (for example, at 5320 Å), it seems likely that inversion and reasonably high gain should be obtainable at 1091 Å.

QUASI-METASTABILITY

In an alkali-like atom or ion in which L and S are good quantum numbers (pure Russell-Saunders coupled eigenfunctions), several classes of core-excited levels are metastable against autoionization. Among the levels in the doublet manifold, the simultaneous conservation of parity and orbital angular momentum L forbids Coulombic autoionization of pure doublet levels having odd parity and even L , or vice versa, even parity and odd L . Another class of metastable levels consists of all pure quartets which lie below the quartet continuum (below the first triplet level in the next stage of ionization). These levels are metastable against autoionization by the requirement of conservation of spin.

The effect of breakdown of L-S coupling due to the spin-orbit interaction is to cause mixing of doublet and quartet levels. From the properties of angular momenta, the spin-orbit interaction term $\mathbf{L}\cdot\mathbf{S}$ connects pure L-S basis states satisfying $\Delta L = 0, \pm 1$; $\Delta S = 0, \pm 1$; and $\Delta J = 0$. This mixing to adjacent L levels has the following effect: doublets that were forbidden to autoionize because of parity and angular momentum considerations are mixed with levels which do autoionize rapidly. Consequently, all doublets tend to autoionize. Similarly, quartets are mixed with doublet levels and thereby acquire both autoionizing and radiative character. Tables I and II give the results of single-configuration calculations, using the atomic physics code[2] RCN/RCG for levels of the $5p^5 5d6s$ configuration in neutral Cs. These calculations indicate, even for levels that in a pure L-S scheme would not undergo Coulombic autoionization, that in general the predominant decay mechanism is autoionization.

Table I Autoionizing and radiative rates for odd parity-even angular momentum doublet levels of the Cs $5p^5 5d6s$ configuration

Upper Level	Autoionizing Rates (sec^{-1})	Radiative Rate (sec^{-1})
$(^1D)\ ^2D_{3/2}$	1.5×10^{12}	2.6×10^8
$(^1D)\ ^2D_{5/2}$	2.5×10^{11}	4.3×10^8
$(^3D)\ ^2D_{3/2}$	6.8×10^{10}	8.4×10^8
$(^3D)\ ^2D_{5/2}$	3.7×10^{12}	2.5×10^8

Table II Autoionizing and radiative rates for quartet levels of the Cs $5p^5 5d6s$ configuration

Upper Level	Autoionizing Rate (sec^{-1})	Radiative Rate (sec^{-1})
$^4P_{1/2}$	1.1×10^{11}	1.8×10^{7}
$^4D_{1/2}$	1.5×10^{13}	8.3×10^{8}
$^4F_{5/2}$	3.7×10^{12}	2.2×10^{8}
$^4P_{5/2}$	5.1×10^{7}	4.3×10^{7}

There exist, however, certain quartet levels in alkali-like systems which in first order couple only to those pure doublet levels which are themselves prohibited from autoionizing; it is these levels that have been termed as quasi-metastable. In second order, they do acquire components of autoionizing doublet levels, and therefore do autoionize; but often sufficiently slowly that the branching ratio for XUV radiation remains large. As an example consider the quasi-metastable $5p^5 5d6s\ ^4P_{5/2}$ level of Cs. In a pure L-S basis, the only doublet levels to which the $^4P_{5/2}$ level has non-zero matrix elements are the singlet and triplet core $^2D_{5/2}$ levels. The coupling to these levels allows $^4P_{5/2}$ to radiate in the XUV, but causes no autoionization. The calculated (RCN/RGN) expansion of the $5p^5 5d6s\ ^4P_{5/2}$ level of Cs is

$$\begin{aligned} {}^4P_{5/2} = &- 0.90\ {}^4P_{5/2} + 0.35\ {}^4D_{5/2} - 0.051\ {}^4F_{5/2} \\ &- 0.24\ ({}^1D)\ {}^2D_{5/2} - 0.14\ ({}^3D)\ {}^2D_{5/2} \\ &- 0.0043\ ({}^1F)\ {}^2F_{5/2} + 0.0016\ ({}^3F)\ {}^2F_{5/2} \end{aligned} \qquad (1)$$

The much smaller $(0.0043)^2$ and $(0.0016)^2$ components of the autoionizing $^2F_{5/2}$ levels which appear in second order through the diagonalization, result in the relatively slow $^4P_{5/2}$ autoionizing rate. As listed in Table II, the level Cs $5p^5 5d6s\ ^4P_{5/2}$ autoionizes at a calculated rate of $5.1 \times 10^7\ s^{-1}$ and radiates on the $5p^5 5d6s\ ^4P_{5/2} \rightarrow 5p^6 5d\ ^2D_{5/2}$ transition at a rate of $4.3 \times 10^7\ s^{-1}$ at a calculated wavelength of 1075 Å.

XUV EMISSION SPECTRUM

Using a pulsed hollow cathode discharge and a McPherson monochromator we have observed the XUV emission spectrum of Cs. As described elsewhere,[3,4] the hollow cathode operated at a voltage of 3 kV, a current of about 300 amps, and a Cs pressure of about 2 torr. The observed emission spectra are shown in Figs. 2 and 3. The strongest features are those of Xe-like Cs^+ at 901.2 and 926.7 Å. The emission at 1091 Å had an intensity typically equal to about 1/6 of the 927 Å line and is identified as the $5p^5 5d6s\ ^4P_{5/2} \rightarrow 5p^6 5d\ ^2D_{5/2}$ transition. This identification is based upon the observed fine-structure splitting

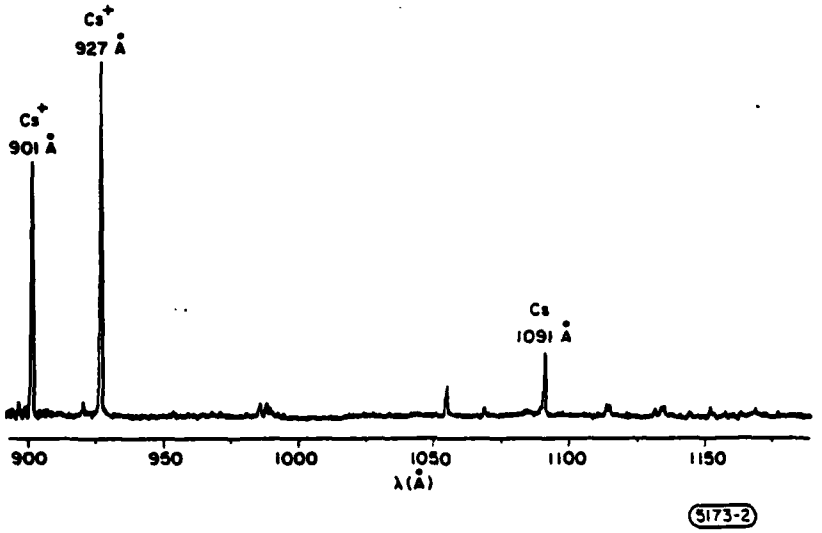

Fig. 2. Emission scan of Cs from pulsed hollow-cathode discharge.

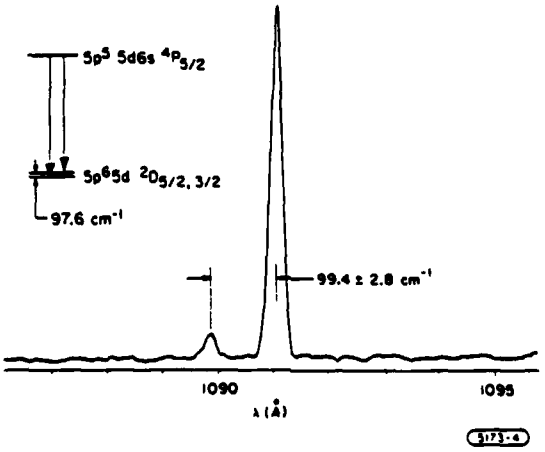

Fig. 3. High resolution scan of Cs near 1091 Å.

of 99 cm^{-1}, corresponding to the splitting of the lower $5p^6 5d\ ^2D_{5/2}$ and $^2D_{3/2}$ levels (Fig. 3); and upon the observed 1/12 intensity ratio of the two components, compared to a ratio of 1/14.3 predicted by the RCN/RGN code.[2] The emission reported here at 1091 Å may or may not be the same as that reported by Aleksakhin, et al.[5] as occurring at 1085 Å.

Cs 1091 Å LASER

Based on the calculated radiative rate, and a Doppler linewidth of 0.15 cm^{-1}, the gain cross section of the 1091 Å laser is 3.9×10^{-14} cm^2. We estimate that our upper level population is somewhere in the range of 10^{11} atoms/cm^3 to 5×10^{12} atoms/cm^3, and therefore the gain for our 30 cm long hollow cathode is between 10% and e^5. Experiments are now underway to determine this number.

A first estimate of the lower level $5p^6 5d\ ^2D_{5/2}$ population is 10^{13} atoms/cm^3. We calculate that a 5320 Å laser with a 5 ns long pulse and a power density of 10^8 W/cm^2 will photoionize atoms in this level and reduce the population by a factor of 5000.

TRANSITIONS FROM QUASI-METASTABLE LEVELS IN OTHER ELEMENTS

Using the code RCN/RGN, we have taken a first look at transitions in other alkali atom and alkali-like ions which originate from quasi-metastable levels.[1]

Table III gives the transition wavelength, Doppler width, and gain cross section σ for XUV laser transitions which originate from the lowest quasi-metastable level of each element. The Doppler width is calculated at a temperature corresponding to a vapor pressure of 10 torr.

Table III Gain cross sections of transitions from quasi-metastable levels

Transition	λ(Å)	Doppler Width (cm^{-1})	σ(cm^2)
Na $2p^5 3s3p\ ^4S_{3/2} \rightarrow 2p^6 3p\ ^2P_{5/2}$	415	1.04	1.6×10^{-16}
K $3p^5 3d4s\ ^4P_{5/2} \rightarrow 3p^6 3d\ ^2P_{5/2}$	711	0.43	4.4×10^{-16}
Rb $4p^5 5s5p\ ^4S_{3/2} \rightarrow 4p^6 5p\ ^2P_{3/2}$	821	0.24	9.1×10^{-15}
Cs $5p^5 5d6s\ ^4P_{5/2} \rightarrow 5p^6 5d\ ^2D_{5/2}$	1075	0.15	3.9×10^{-14}
Mg^+ $2p^5 3s3p\ ^4S_{3/2} \rightarrow 2p^6 3p\ ^2P_{3/2}$	256	1.78	8.71×10^{-17}
Ca^+ $3p^5 3d4s\ ^4P_{5/2} \rightarrow 3p^6 3d\ ^2D_{5/2}$	529	0.83	1.72×10^{-16}
Sr^+ $4p^5 4d5s\ ^4P_{5/2} \rightarrow 4p^6 4d\ ^2D_{5/2}$	620	0.45	5.6×10^{-15}
Ba^+ $5p^5 5d6s\ ^4P_{5/2} \rightarrow 5p^6 5d\ ^2D_{5/2}$	771	0.27	2.4×10^{-14}

ACKNOWLEDGEMENTS

The authors gratefully acknowledge helpful discussions with J. Reader, T. Lucatorto, A. Mendelsohn, K. Pedrotti, J. Spong, and J. F. Young. The work described here was supported by the U.S. Air Force Office of Scientific Research and the U.S. Army Research Office.

REFERENCES

1. S. E. Harris, D. J. Walker, R. G. Caro, A. J. Mendelsohn, and R. D. Cowan, "Quasi-Metastable Quartet Levels in Alkali-Like Atoms and Ions," Opt. Lett. (to be published).
2. Robert D. Cowan, The Theory of Atomic Structure and Spectra (University of California Press, Berkeley, 1981), Secs. 8-1, 16-1, and 18-7.
3. R. W. Falcone and K. D. Pedrotti, Opt. Lett. 7, 74 (1982).
4. R. W. Falcone, D. E. Holmgren, and K. D. Pedrotti, in Laser Techniques for Extreme Ultraviolet Spectroscopy, R. R. Freeman and T. J. McIlrath, eds. (AIP, New York, 1982).
5. I. S. Aleksakhin, G. G. Bogachev, I. P. Zapesochnyl, and S. Yu. Ugrin, Sov. Phys. JETP 53, 1140 (1981).

END

FILMED

4-85

DTIC